



## The role of backstop shape during inversion tectonics physical models

CAROLINE J.S. GOMES, ANDRÉ DANDERFER FILHO,  
ANA MARIA A. POSADA and ANIELLE C. DA SILVA

Universidade Federal de Ouro Preto, Escola de Minas, Departamento de Geologia, Morro do Cruzeiro, s/n  
35400-000 Ouro Preto, MG, Brasil

*Manuscript received on May 5, 2009; accepted for publication on June 22, 2010*

### ABSTRACT

The style of deformation of rocks from basin-infilling sequences in positively inverted natural basins was discussed upon the results of laboratory experiments carried out in sandboxes with sand packs laid down in the space between two wooden blocks. The space simulated stages of crustal extension leading to (1) a half graben due to extension above a listric extensional detachment, with the blocks simulating the footwall and hanging wall, or (2) a graben, with the blocks simulating the external margins that drifted apart above a horizontal detachment. Combinations of two different angles were used to simulate the dip of curved normal faults along the internal face of the wooden blocks. Backstops in the half graben had a convex up internal face. Backstops in the graben had a concave up internal face. Shortening was partitioned in forward and backward movements within the sand packs, and the kinematics of contraction was largely influenced by the convex or concave internal faces. A buttress effect characterized by rotation of the sand pack close to the footwall was stronger for footwall with steeper-dipping internal faces. The results were compared to other physical experiments and applied to an inverted basin found in nature.

**Key words:** analogue models, backstop geometry, buttress effect, inversion tectonics, normal detachment reactivation.

### INTRODUCTION

The geometry and tectonic features of inverted basins have been described since the beginning of the century. However, the formal definition of 'inversion' was only presented in 1981 by Glennie and Boegner (1981). According to these authors, 'inversion' represents the reversal of the regional stress regime, from extension to contraction, or the opposite. Cooper et al. (1989) suggest that the inversion process should involve: basin formation by normal faulting, sedimentation and subsequent compression or transpression causing uplift and partial extrusion of the basin infill.

Inversion in orogenic belts involves deformation of continental margin prisms and is normally characterized by thin- and thick-skinned thrust sheets and nappes.

This inversion style produces major crustal shortening and was discussed by several authors dealing with foreland fold-thrust belts such as the Appalachians, the Rocky Mountains, the Alps and the Himalayas (respectively in Mitra 1988, de Graciansky et al. 1989, Hayward and Graham 1989, Jadoon et al. 1994).

According to Glen et al. (2005), three different tectonic models may be used to reproduce inversion: a) the fault-reactivation model; b) the thin-skinned model; and c) the buttress model. The first model postulates that reactivation preferentially occurs along faults that have the lowest dip angle or the lowest resistance to forward movement. In the 'thin-skinned model', inversion develops by the formation of new thrust faults rather than by reactivation of pre-existent normal faults. Finally, in the 'buttress model', inversion is controlled by the rheologic contrast between the basement and syn-rift sedimentary sequences. According to Butler (1989)

Correspondence to: Caroline Janette Souza Gomes  
E-mail: caroline@degeo.ufop.br

and Hayward and Graham (1989), the basement, either in the hanging wall or in the footwall of the extensional detachment, may produce buttressing structures in the syn-rift sequence either by folding and associated cleavages, rotation in the foreland or backward propagating displacements.

Despite several analogue experiments have demonstrated how do structures progressively develop during inversion, according to the fault-reactivation and the thin-skinned models (respectively McClay 1995, 1989), the buttress effect does not appear to have been conveniently addressed, and we think that the geometry of the backstop may play a fundamental role in the deformation pattern of the basin infill, as well as in the reactivation of the basal detachment. Thus, we carried out a series of analogue experiments in sandboxes in order to analyze the buttressing effects (rotation in the foreland and/or backward propagating movement) and the conditions of reactivation of the normal detachment. We label as backstop the rigid mass that moves on the basal detachment to cause contraction of the basin-infilling sequences, whereas the term buttress refers to a rigid mass that restrains the dislocation of the thrust sheets. Both the backstop and the buttress have the ability to support larger deviatoric stresses than the basin-infilling sequences.

In the evolution of orogenic wedges, backstops (or indenters) have been described both in analogue (e.g., Mulugeta 1988, Bonini et al. 1999) and numerical models (e.g., Byrne et al. 1993, Beaumont et al. 1994). Byrne et al. (1993) consider a backstop as a structural domain that bears strong differential stresses and generates a deformation front similar to a bulldozer pushing from behind an accretionary wedge. According to these authors, a backstop plays a key role in the geometry of an accretionary wedge on a subduction zone. A foreland-dipping backstop for instance causes, among other features, the growth of a high outer arc and thrust vergence inversion.

In our study, we described analogue models in which the deformable hanging wall of a basin is inverted by stiff, convex-up and concave-up backstops (Fig. 1). The convex-up and concave-up geometries refer to the curvature of the foreland-dipping face of the backstop that is unconformably covered by the basin infill (Fig. 1i

and 1ii, respectively). The convex-up backstop simulates the hanging wall block above a listric extensional detachment (Fig. 1i); the concave-up backstop simulates any of the two margins of a graben; in other words, it is a block that can be moved on a horizontal detachment (Fig. 1ii). In addition, we investigated the effect of two different angles of dip for the foreland-dipping face of the backstop and the rigid block (termed normal footwall block) on the style of deformation of the basin infill.

## DESCRIPTION OF THE EXPERIMENTS

### SCALING

For the analogue experiments to be valid, model parameters must be properly scaled. Hubbert (1937) established scaling relationships between the geometric, kinematic, and dynamic properties of the models and the corresponding properties of the geological counterparts. The scale of model-prototypes is determined by three basic parameters: length, time and mass. For geometrically and kinematically similar structures, the dynamic similarity requires that the ratio between forces in model and prototype must be constant if compared kind to kind. From this condition follows another one: the ratio between two dissimilar forces in the model must be equal to the ratio between the same two forces in the prototype. For our purpose, the most significant force ratio is gravity force ( $F_g$ ) / pressure force ( $F_p$ ), written as follows:

$$\rho l^3 \mathbf{g} / \Delta\sigma \times l^2 \quad \text{or} \quad \rho l \mathbf{g} / \Delta\sigma \quad (1)$$

where,  $\rho$  = rock density,  $l$  = length,  $\mathbf{g}$  = gravity on Earth surface, and  $\Delta\sigma$  = rock strength. From the above requirement and expression (1) follows that

$$(\rho l \mathbf{g} / \Delta\sigma)_{\text{model}} = (\rho l \mathbf{g} / \Delta\sigma)_{\text{prototype}} \quad (2)$$

Once the density of the materials has little influence in the solution of equations 1 and 2, and the gravity field in experiments and nature is the same, equation 2 can be rewritten as

$$(l / \Delta\sigma)_{\text{model}} = (l / \Delta\sigma)_{\text{prototype}} \quad \text{or} \\ l_{\text{model}} / l_{\text{prototype}} = \Delta\sigma_{\text{model}} / \Delta\sigma_{\text{prototype}}.$$

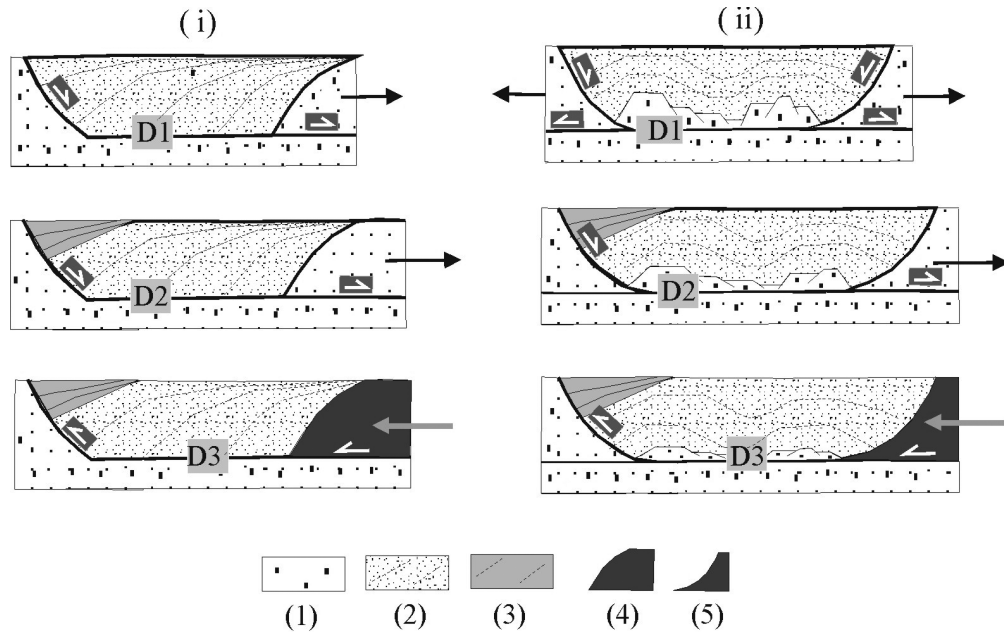


Fig. 1 – Conceptual cartoon showing the authors idea for the positive inversion of a half graben (i) and a graben (ii) by sliding a mobile block above listric or horizontal basal detachments, respectively. Arrows indicate the sense of displacement of the moving walls, and D1, D2 and D3 the active detachments along time. (1) basement; (2) syn-rift 1; (3) syn-rift 2; (4) convex-up backstop, and (5) concave-up backstop during inversion.

Thus, if the length in the model is decreased by a scale factor  $\lambda = 10^{-5}$ , the ratio of cohesive strength  $\sigma_r$  must be decreased also by  $10^{-5}$ . Equation 2 justifies the use of dry sand as analogue material in several experiments, because a reduction of the original by 100.000 times requires that the analogue material has cohesive strength close to zero.

The cohesive strength of sand has been subject of discussion. A common method used to estimate the strength of sand under low normal stresses consists of a linearly extrapolation from measurements made at higher values, yielding a wide range of results between 12 and 500 Pa. Eisenstadt and Sims (2005) noted that the cohesive strength of sand is low but increases with higher levels of ambient humidity. They evaluated sand and clay models used to simulate deformation in brittle rocks and concluded that neither is perfect for scaled modeling, but both reproduce remarkably well the deformation patterns of the upper crust. In our scaled models, we selected quartz sand as analogue material due to its ease of construction and dissection.

Sand is considered to behave as a Mohr-Coulomb material similar to the upper brittle crust that implies a friction angle of about  $30^\circ$  and a time-independent de-

formation. Therefore, the ratio between length and time is an independent ratio, enabling us to choose a suitable ratio for our experiments. The models were deformed by displacing the mobile wall, driven by a motor, at a rate of  $2 \times 10^{-3}$  cm/s (2 cm/h). The adopted scale factor was  $10^{-5}$  and, consequently, a 5-cm height in the model represented 5 km of brittle crust in the prototype.

#### EXPERIMENTAL SET-UP

Our experiments were carried out at the Laboratory of Tectonic Modelling of the Department of Geology, Federal University of Ouro Preto (Brazil). During laboratory work, 16 series of experiments were performed in order to study the effect of mobile backstop curvature on contraction and on positive inversion, with variable initial lengths. Only the positive inversion deformation experiments are presented and discussed here. In the sandboxes, the space between the backstop and the normal footwall was filled with fine layers of sand of different colors (sand pack 1, Fig. 2). The models were 5 cm deep, 20 cm wide, and the initial length between the rigid backstop toe and the rigid normal detachment footwall toe was 14 cm. All experiments were run in two successive steps. In the first step, 6 cm of exten-

sion (42.9%) was applied to the hanging wall with syn-extension sedimentation (sand pack 2). At the end of the extension, the top surface of the experiment was covered with an additional thin horizontal layer to visualize the compressional deformation. In the second step, the extensional basin was submitted to a 12-cm contraction (60%). Therefore, the final length between backstop and normal footwall toe was 8 cm.

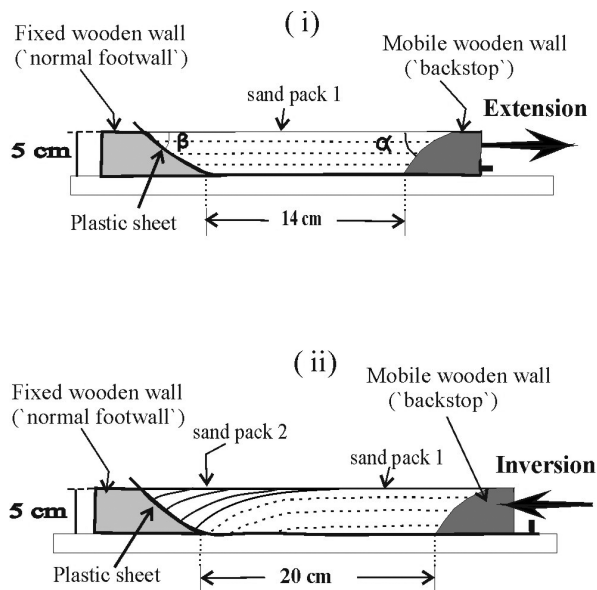


Fig. 2 – Schematic illustrations of the experimental apparatus for sequence 1 (in sequences 2 and 3 the backstop is concave-up and vertical, respectively). (i) Apparatus before extension, and (ii) apparatus after extension and before inversion. Sand pack 1 represents the rift infill during the oldest extension event (also named syn-rift 1) (not simulated), and sand pack 2 represents the syn-rift deposit of the second extension event (also named syn-rift 2) – our first deformation step.  $\alpha$  and  $\beta$  are the backstop and the normal footwall cut-off angles, respectively.

Three experimental sequences were set up, and in two of them we changed the backstop curvature, from convex upward (sequence 1) to concave upwards (sequence 2). In these sequences, the backstop cut-off angle ( $\alpha$ ) and the normal footwall cut-off angle ( $\beta$ ) were either  $60^\circ$  or  $70^\circ$ , which are the angles usually found in nature (models 1-8, Table I). Sequence 3 consisted of two experiments (9 and 10) with a plane, vertical mobile wall in order to compare the results with traditional experiments (e.g., Buchanan and McClay 1991). In these

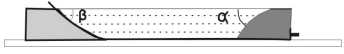



experiments, backstops were not characterized by any specific lithology or geological body, and may be understood as the result of lateral increase in strength compared to the foreland.

For all experiments (Table I), the layers of colored homogenous sand were deposited on a plastic sheet that simulates a low friction basal detachment (normal detachment D2; Fig. 2i). The plastic sheet overlays the wooden normal footwall and passes under the backstop where it was attached. Prior to inversion, the plastic sheet was detached from the mobile wall, but remained in the experimental box to simulate a possible reactivation of the normal detachment (detachment D2 = D3, Fig. 2ii). Photographs that were taken through the transparent sidewalls recorded the evolution of the structures at regular intervals. In addition, at the end of the inversion, the sand models were strengthened by infusion with water, then cut and photographed. We observed that friction between the sand and the glass sides caused a minor slip of the fault-blocks at the sidewalls with respect to the sand pack center. This means that the lateral shear stress actually interferes with the model evolution, but it does not modify the overall structural architecture.

#### EXPERIMENT LIMITATIONS

Because our experiments involve some simplifications, they have limitations that require a critical analysis, such as physical modelling experiments in general. A limitation of our analogue experiments relates to the material discontinuity between sand packs 1 and 2 and the wooden blocks simulating the backstop and the normal footwall. Sand packs 1 and 2 are mechanically equal. The physical discontinuity produced a mechanically defined basal detachment that highly controlled the deformation trajectory. In natural structures, fluid pressure may greatly enhance reactivation by lowering resistance along the fault zone. Cobbold et al. (2001) demonstrated that the style of deformation in sandboxes could be partially controlled by the amount of fluid pressure. However, pore fluid pressure effects were not taken into account in our experiments. We believe that the main potential of physical modelling is to provide a visual image of progressive deformation under different combinations of controlling parameters, while in the real world only the final deformation product is available.

**TABLE I**  
Summary of boundary conditions of our 10 experiments.

SEQUENCE / MODEL NUMBER		NORMAL FOOTWALL	BACKSTOP
		Dip angle ( $\beta$ )	Dip angle ( $\alpha$ )
Sequence 1: Convex-up mobile backstop 	1	60°	60°
	2	60°	70°
	3	70°	60°
	4	70°	70°
Sequence 2: Concave-up mobile backstop 	5	60°	60°
	6	60°	70°
	7	70°	60°
Sequence 3: Vertical mobile backstop sand pack height = backstop height (SPH = BH) 	9	60°	90°
	sand pack height < backstop height (SPH < BH) 	10	60°

Finally, our experiments did not account for potential thermal effects, compaction and isostatic adjustment. Some other limitations involve constant extension and convergence angle, and rate of deformation. In nature, variations in both parameters may affect the geometry of the structures and the mechanics involved in their formation.

Our simplified approach is justified by the purpose of providing basic guides for understanding inversion tectonics when basin closure is caused by stiff, convex-up and concave-up backstops.

**RESULTS**

For all experiments presented below, we described progressive deformation stages of one extensional experiment (model 1) and two inversion models: one convex-up (again model 1) and one concave-up (model 6) mobile backstop sequence. In the other experiments we focused only on the end results of inversion, which were

illustrated by cross-sections cut through the central region of the experiments.

EXTENSIONAL EXPERIMENT

The progressive extension in experiments with convex-up backstop and dip angles of 60° resulted in a sequence of structures that compares well with the typical sequence observed in physical experiments of extension (McClay 1990). Characteristic features in sand pack 1 (syn-rift 1) are a gentle flexure in the hanging wall after 14,3% (2 cm) of extension (Fig. 3ii), and the successive development of normal faults to form a crestal collapse graben within the roll-over anticline (Figs. 3iii-iv). Two antithetic (E1 and E2) and one synthetic (E3) normal faults bounded the crestal collapse graben after 42,9% (6 cm) of extension.

The progressive extension with footwall block cut-off angle  $\beta = 70^\circ$ , in experiments 3, 4, 7 and 8 (not shown), produced at the final extension i) a crestal col-

lapse graben with a greater number of normal faults (up to four), and ii) a higher counterclockwise rotation of the syn-rift sand pack 1 close to the footwall.

#### INVERSION EXPERIMENTS WITH A CONVEX-UP MOBILE BACKSTOP

##### *Inversion steps – Model 1 ( $\alpha$ and $\beta = 60^\circ$ )*

The successive stages of inversion are presented in Figure 4 (i to iv). After 20% of shortening (4 cm), a box fold-type structure has developed next to the backstop with limbs corresponding to a forethrust (F1) and a backthrust (B1). With the progressive deformation (40% = 8 cm), the sand wedge was pushed up and carried backward (to the right) up the backthrust B1, and a second forethrust (F2) developed when slip on forethrust F1 ceased.

After 60% of shortening (12 cm) (Fig. 4iv), the box fold became an asymmetric ramp anticline onto the convex-up backstop, because the compressional fault system (F1 + F2) was carried up and backward relative to the movement of the backstop. Such movement gave origin to forethrust F3 that formed right at the toe of the backstop and increased deformation of the crestal collapse graben. The sand pack 2 (syn-rift 2) thickened slightly nearby the footwall and started to be pushed up and out of the half graben, but the basal detachment did not reactivate. The crestal collapse graben fault system was cut by forethrust 2 and 3 and underwent rotation and narrowing (Fig. 4iv).

##### *End results: Models 1 to 4*

Figure 5 presents the profile line drawings of the central region of models 1 to 4, at final shortening. In all the experiments, at least three forethrusts cut the normal faults in the foreland, and a major rotation of the crestal collapse graben system occurred.

The main difference between models 1 and 3 ( $\alpha = 60^\circ$ ) and models 2 and 4 ( $\alpha = 70^\circ$ ) concerns to the deformation in the sand pack close to the backstop. In the latter, the high backstop angle produced after 40% of shortening (not shown) a second backthrust (B2) below the first one. The difference between models 1 and 2 ( $\beta = 60^\circ$ ) and 3 and 4 ( $\beta = 70^\circ$ ) concerns to the amount of counterclockwise rotation of the syn-rift sand pack 1

close to the footwall (Figs. 5 and 6i). Such rotation is the greatest in experiment 4, in which the internal face of both the normal footwall and the backstop dip steeply.

Reactivation of the normal detachment did not occur in any of the experiments, because the backstop geometry allows an intense backward movement of the sand wedge. Consequently, all profiles showed a ramp anticline on the backstop, the hinges varying from rounded (experiments 1 and 3) to flattened (experiments 2 and 4). Excepting experiment 1, both the backward displacement (termed S) on the backstop flat and the ratio between S and the fold amplitude (A) were almost constant (Figs. 7i and 8i).

#### INVERSION EXPERIMENTS WITH A CONCAVE-UP MOBILE BACKSTOP

##### *Inversion steps – Model 6 ( $\alpha = 70^\circ$ and $\beta = 60^\circ$ )*

The concave-up backstop caused a deformation trajectory different from that observed for the convex-up backstop. Most of the deformation was accommodated by the rise and backward movement of the sand wedge relative to the transport of the backstop, which produced a pronounced ramp anticline (Fig. 9). After 20% of shortening (4 cm), forethrust F1 appears (and backthrust B1), and after 40% of shortening (8 cm), forethrust F2 is formed together with a second backthrust (B2). Thrust F2 cuts normal fault E1. After 50% of shortening (10 cm) (not shown), F2 becomes locked, and as a consequence, the normal detachment is reactivated (Fig. 9 iv). In this process, the crestal collapse graben becomes narrower.

##### *End results: Models 5 to 8*

The line drawings of profiles across the center of experiments 5 to 8 are presented in figure 10. Due to the larger area between the two wooden blocks, the movement of the concave-up backstops produces a less intense deformation in this sequence. Rotation of the crestal collapse graben system is small, and with the exception of model 8, only two thrust faults are observed. Backthrusts formed at the right side of the model. In model 8, forethrust F3 extends to the syn-rift sand pack 2 cutting the normal fault E3 after a short dislocation parallel to it. Close to fault F3, two backthrusts of minor expression are formed at the base of the sand wedge.

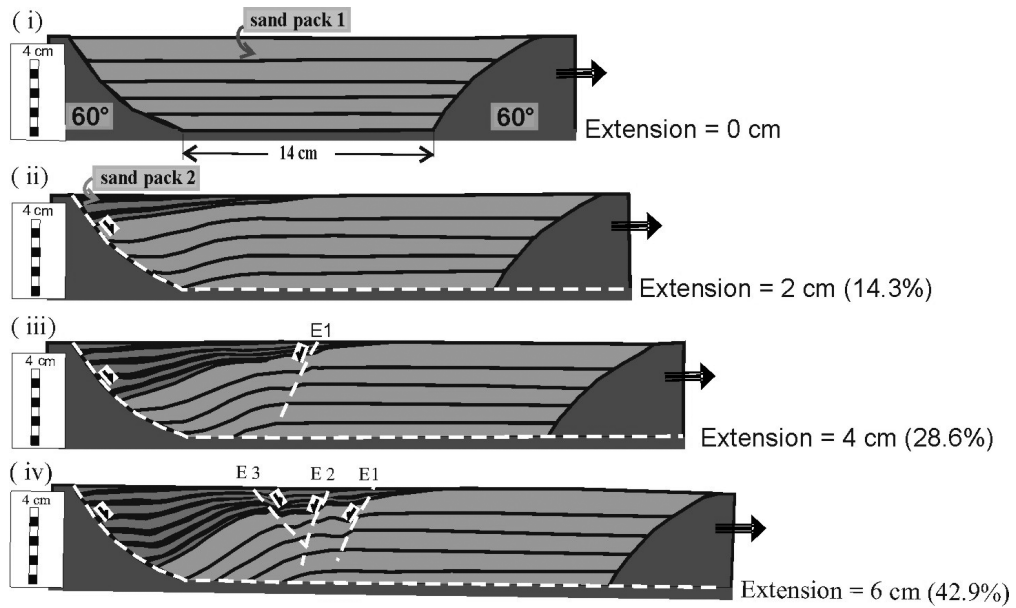


Fig. 3 – (i-iv) Sequential line drawings of extensional steps of photographs that were taken through the transparent sidewalls of model 1 ( $\alpha$  and  $\beta = 60^\circ$ ) showing normal fault sequence E1-E3.

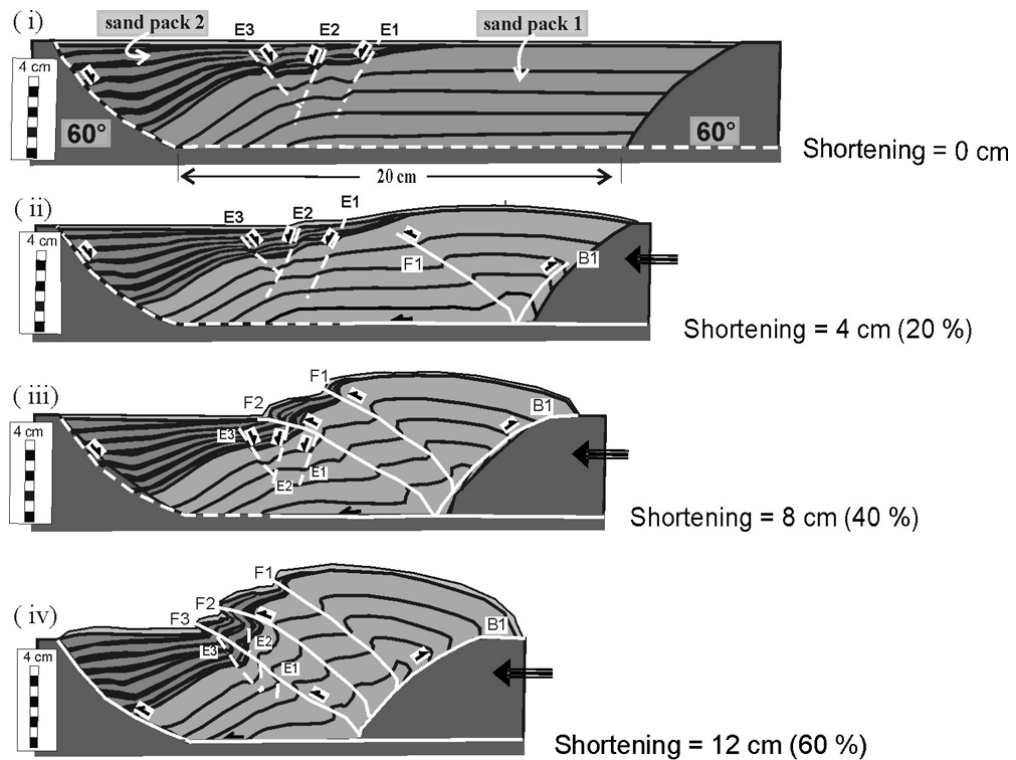


Fig. 4 – (i-iv) Sequential line drawings of inversional steps of photographs taken through the transparent sidewalls of model 1 ( $\alpha$  and  $\beta = 60^\circ$ ). E1-E3 are structures that were formed during extensional steps; F1-F3 are forethrusts, and B1, a backthrust. Dashed and continuous lines represent extensional and compressional structures, respectively.

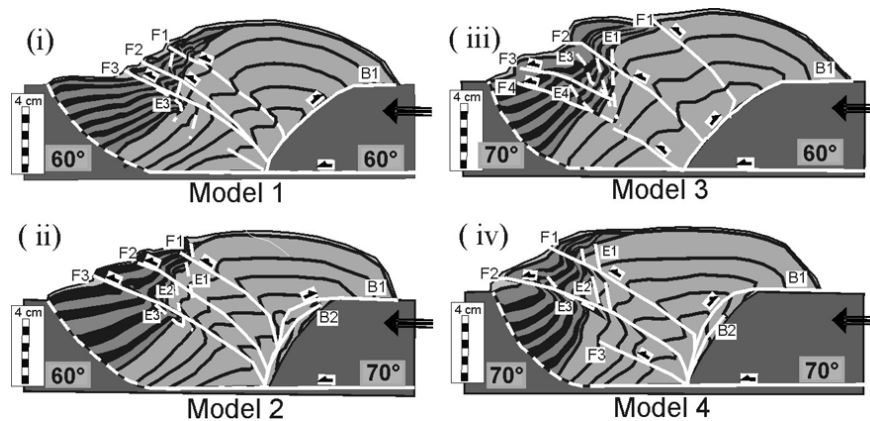


Fig. 5 – (i-iv) Line drawings of cross-sections cut through the central region of models 1 to 4: end results. E1-E3 are normal faults that were formed during extensional steps; F1-F3 are forethrusts, and B1 and B2, backthrusts. Dashed and continuous lines represent extensional and compressive structures, respectively.

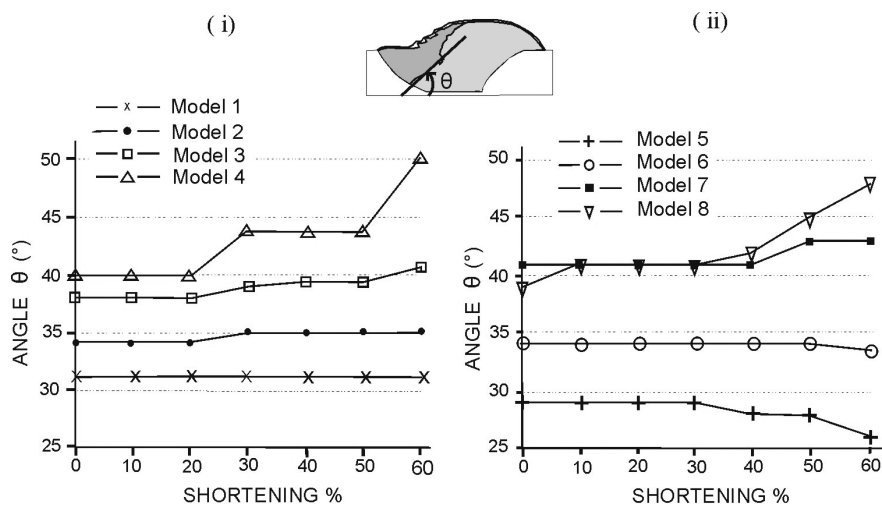


Fig. 6 – Plot of the angle between layering in the sand pack and the normal detachment (angle  $\theta$  shown in the inset) vs. shortening (%) for the inversion experiments with (i) a convex-up mobile backstop (models 1 to 4) and (ii) a concave-up mobile backstop (models 5 to 8). Experiments with a steep-dipping normal detachment ( $\beta = 70^\circ$ ; experiments 3, 4, 7, and 8) produced greater counterclockwise rotation of the sand pack.

The difference between the results of experiments 5 and 6 ( $\beta = 60^\circ$ ) and experiments 7 and 8 ( $\beta = 70^\circ$ ) concerns the reactivation of the normal detachment in the former two and a bigger backward displacement in the latter two (Figs. 10 and 7ii). As in the case of the inversion experiment with a convex-up mobile backstop, the steeper normal detachment cut-off angle in models 7 and 8 caused a pronounced counterclockwise rotation of the syn-rift sand pack 1 (Fig. 6ii). Comparing the end results of models 5 ( $\alpha = 60^\circ$  and  $\beta = 60^\circ$ ) and 6 ( $\alpha = 70^\circ$  and  $\beta = 60^\circ$ ), different amounts of forethrusts slip and normal detachment reactivation are depicted (Figs. 10i

and ii). Model 7 differs from model 8 in the deformation style: the backward displacement on backstop flat is larger in model 7 (Fig. 7ii), and the number of faults and respective dip slip is larger in model 8 (Fig. 10iv).

#### INVERSION EXPERIMENTS WITH A VERTICAL MOBILE BACKSTOP

##### End results – Models 9 and 10

Figure 11 shows line drawings of model 9, set up with equal sand pack and backstop heights (SPH = BH). The final deformation reveals a strong normal detachment



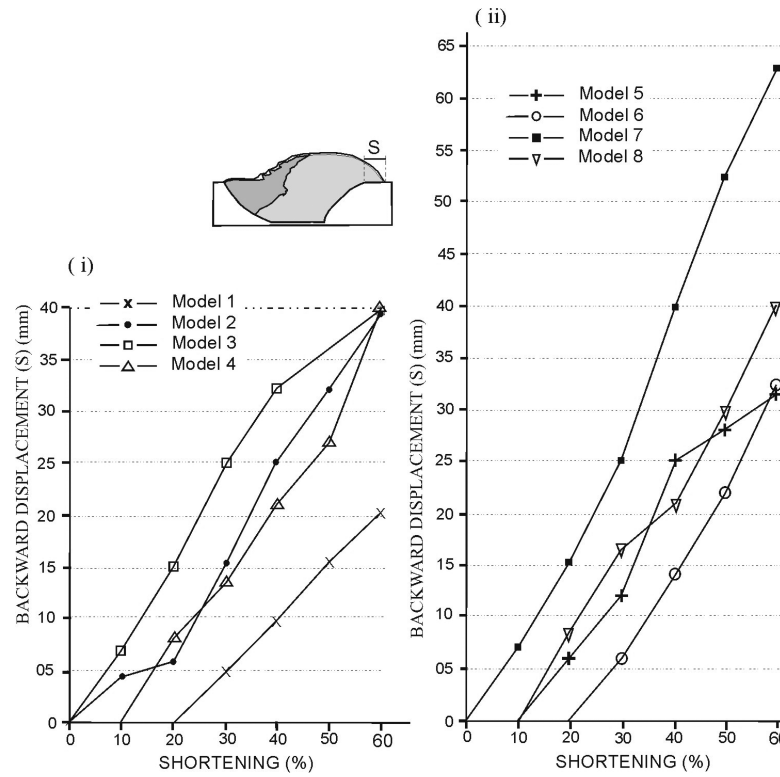


Fig. 7 – Plots of backward displacement on backstop flat (S) (see inset cross-section) vs. shortening (%) for the inversion experiments with (i) a convex-up mobile backstop (models 1 to 4) and (ii) a concave-up mobile backstop (models 5 to 8). The concave-up mobile backstop model 7 produces the highest backward displacement due to its high normal detachment cut-off angle and its low backstop cut-off angle.

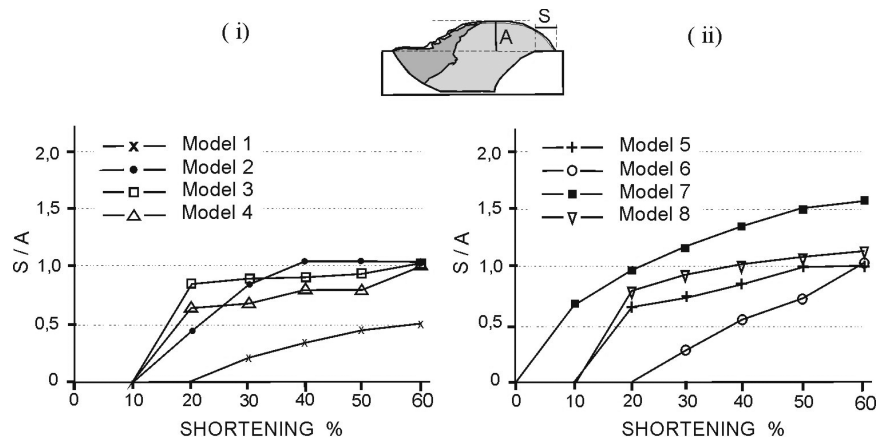


Fig. 8 – Ratio of backward displacement on backstop flat (S) vs. anticlinal amplitude (A) (see inset cross-section) plotted against shortening (%) for the inversion experiments with (i) a convex-up mobile backstop and (ii) a concave-up mobile backstop. The convex-up mobile backstop model 1 ( $\alpha$  and  $\beta = 60^\circ$ ) and the concave-up mobile backstop model 7 produce the smallest and biggest S/A ratio, respectively (see text for explanation).

reactivation. Moreover, two backthrusts (B1 and B2) and two forethrusts (F1 and F2) formed. The progressive deformation (not shown) started almost concomitantly in the hinterland, the center and the foreland by

sand pack thickening close to the backstop, slight rotation of the antithetic normal faults (clockwise) and normal detachment reactivation, respectively. Only after 40% of shortening, the forethrusts (F1 and F2) formed.

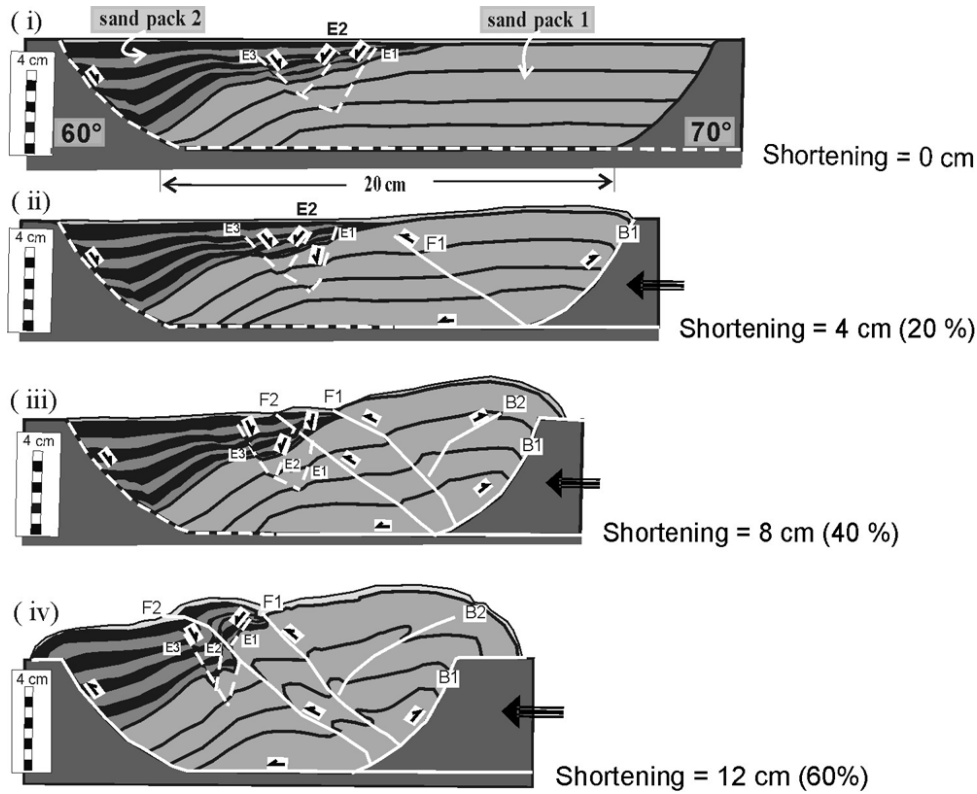


Fig. 9 – (i-iv) Sequential line drawings of inversion steps of photographs that were taken through the transparent sidewalls of model 6 ( $\alpha = 70^\circ$  and  $\beta = 60^\circ$ ). E1-E3 are structures formed during extensional steps; F1 and F2 are forethrusts, and B1 and B2, backthrusts. Dashed and continuous lines represent extensional and contractional structures, respectively.

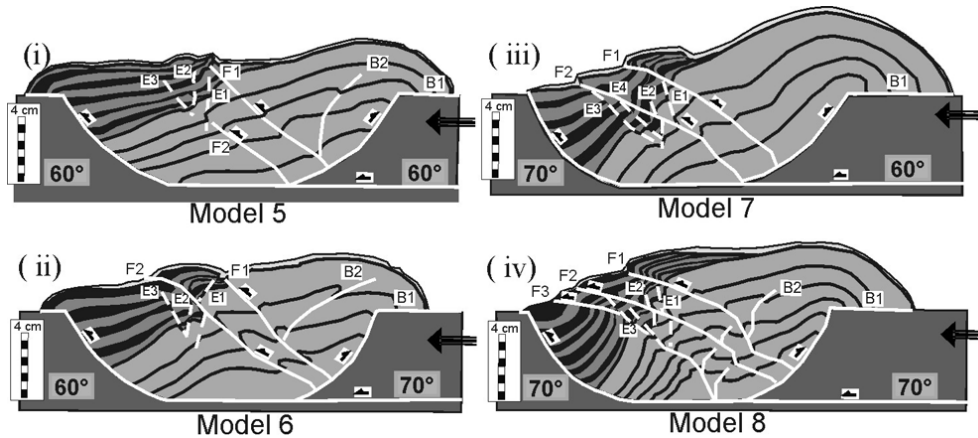


Fig. 10 – (i-iv) Line drawings of cross-sections cut through the central region of models 5 to 8: end results. E1-E4 are normal faults formed during extensional steps; F1-F3 are forethrusts, and B1 and B2, backthrusts. Dashed and continuous lines represent extensional and contractional structures, respectively.

In model 10 (SPH<BH) (Fig. 12), also occurred a strong reactivation of the normal detachment. The higher backstop produced a small increase in the vertical ejection of the sand pack when compared to the

vertical ejection observed in experiment 9 (a difference of 0,4 mm, in Fig. 13). However, the increase in SPH is not proportional to the increase in the BH. One forethrust (F1) formed at the toe of the vertical backthrust.

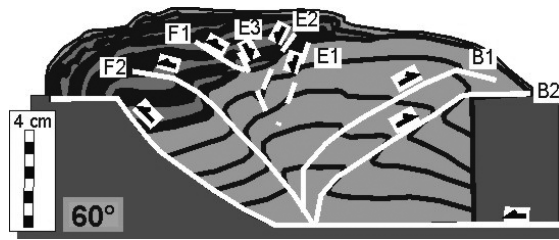


Fig. 11 – Line drawing of a cross-section cut through the central region of model 9: end result. E1-E3 are normal faults formed during extensional steps; F1 and F2 are forethrusts, and B1 and B2, backthrusts. Dashed and continuous lines represent extensional and contractional structures, respectively.

After 50% of shortening (not shown), forethrust F1 was dislocated by backthrust B1 at the middle of the profile (Fig. 12). One more backthrust (B2) was produced at the normal footwall toe, and a forethrust (F2) formed beneath the crestal collapse graben, in the foreland.

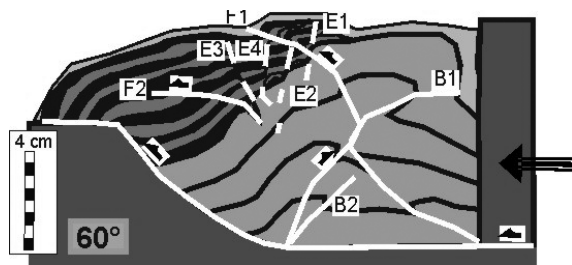


Fig. 12 – Line drawing of a cross-section cut through the central region of model 10: end result. E1-E4 are normal faults formed during extensional steps; F1 and F2 are forethrusts, and B1 and B2, backthrusts. Dashed and continuous lines represent extensional and contractional structures, respectively.

**DISCUSSION**

**COMPARISON AMONG THE RESULTS OF THE EXPERIMENTS**

In all models (1 to 10), 60% of shortening caused vertical ejection associated with back and/or forward horizontal extrusion. The sense of the horizontal displacement depends on the morphology, dip angle and height of the adjacent blocks, particularly of the backstop.

Figure 13 compares deformation in the 60°-dipping footwall models (models 1, 5, 9 and 10) with the variable geometry of the backstop at final shortening (60%). The results reveal that all models with SPH = BH, independent of the backstop geometry, generated a back-

ward movement, and the magnitude of movement is controlled by the backstop geometry. The backward movement is smaller when the backstop is vertical, and bigger when concave. In both experiments with vertical backstops (Figs. 13iii and iv), a strong normal detachment reactivation is noticed (from 20% shortening on), whereas in experiments with curved backstop, only the models with concave-up backstop produced reactivation (starting at 40% of shortening). Moreover, at the end of the deformation, the height of the deformed sand pack is almost the same in all experiments (Figs. 13i-iv), differing only in the back- and forward slip magnitudes. It is important to stress out that none of the crestal collapse graben normal faults underwent reactivation in our models. Excepting models 5, 9 and 10, these faults are transected by the forethrusts.

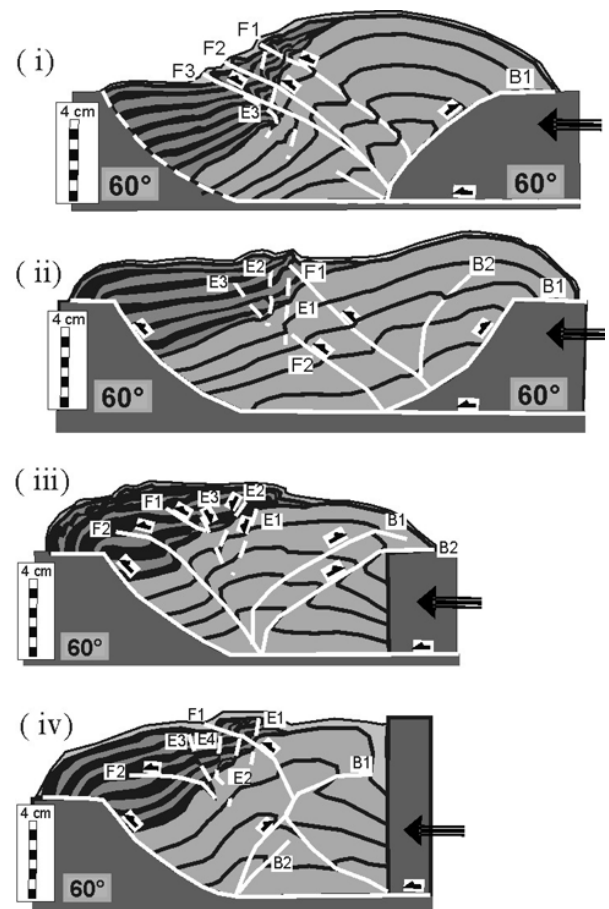


Fig. 13 – Models (i) 1, (ii) 5, (iii) 9 and (iv) 10, with the same 60°-dipping footwall but with different backstop geometries for comparison of thrust patterns.

Finally, the models demonstrated that the combined effect of the normal footwall stiffness and the high dip angle ( $70^\circ$ ) of the bounding normal detachment causes a buttress effect by rotation of the syn-rift pack close to the extensional detachment (models 3, 4, 7 and 8). Graphics in Figure 6 demonstrate that, in models 1, 2, 5 and 6 ( $\beta = 60^\circ$ , Table I), the angle between layering in the sand pack and the normal detachment (angle  $\theta$  shown in the inset of Fig. 6) stayed low during all the inversion steps (between  $29^\circ$  and  $34^\circ$ ), while in experiments 3, 4, 7, and 8 ( $\beta = 70^\circ$ , Table I), the angle  $\theta$  started close to  $40^\circ$ , and in models 4 and 8 the sand pack rotated counterclockwise for nearly  $10^\circ$ .

#### COMPARISON WITH PREVIOUS EXPERIMENTAL MODELS AND WITH A GEOLOGICAL EXAMPLE

##### *The backstop*

Mulugeta and Koyi (1987) and Gomes (1996) discussed the effect of a vertical mobile wall on the compressive structures in sand models. The vertical and stiff wall causes strong ejection of the analogue material close to the backstop, together with backthrusting and verticalization of the older compressive faults as well, as a progressive decrease in the spacing between the thrust faults.

Rossetti et al. (2002), among others, studied, by means of thermomechanical laboratory experiments, the formation of accretionary wedges (traction-reversal models) in subduction zones, varying the backstop geometry and convergence velocities. The authors used viscous paraffin ( $T \geq 37^\circ$ ) to simulate the crust, and demonstrated that the above factors controlled the position of the axial ridge of the wedge and the propagation of the deformation front.

Bonini et al. (1999) described physical sand models and demonstrated that indenters (or backstops) with a low-angle ( $\leq 60^\circ$ ) ramp geometry cause upward and backward movement of sand packs. Indenters with  $60^\circ$ -dipping ramps cause the formation of isolated backthrusts, and in experiments with steeper ramp angles ( $> 60^\circ$ ), the backward movement occurs on backthrusts rather than along the backstop. Continuous displacement results in the formation of thrusts with double vergence. Our experiments showed the same result solely for concave-up backstops. Our experiment with con-

vex-up backstops generated different final results, with backward rise initially occurring on a backthrust, as in the experiments with  $> 60^\circ$ -ramp geometry reported by Bonini et al. (1999). However, with the progressive deformation in our experiments, the more the backstop was pushed forward, the more the backthrust got closer until the backstop touched it. In the following steps of the experiment, the sand pack rose in such a way that the ascension seemed to occur along the backstop itself.

Field evidences of backward movement in inversion tectonics environments are not common. In the northern precambrian Espinhaço Basin, on the eastern margin of the São Francisco Craton, Abad Posada (unpublished data) described an inversion process with reactivation of normal detachments, buttressing effect (counterclockwise rotation of the syn-rift pack) and backward shearing along the eastern basement block (Fig. 14). We noticed that, despite the absence of forethrusts, the bulk deformation pattern in the cross-section of Figure 14, which was constrained on line-length balancing and restoration to the horizontal, is in good agreement with our experimental models with the concave-up backstops (compare, for example, Figs. 14 and 10iv).

##### *The fault reactivation*

According to Brun and Nalpas (1996), sand models with deformable footwall and hanging wall blocks require a strike-slip component to the reactivation of preexisting normal faults. Panien et al. (2005) demonstrated that inversion achieved with deformable footwall and hanging wall blocks produces forethrusts and backthrusts that cut across extensional faults, whereas reactivation is a minor process. Eisenstadt and Sims (2005) compared inversion produced by dry sand and wet clay and concluded that, independently of boundary conditions, the inversion in analogue models is rheologically sensitive. Whilst in dry sand models it causes essentially uplift by sets of conjugate thrusts and minor reactivation of pre-existent faults, in wet clay models normal fault reactivation prevails regardless of fault dip, probably due to high fluid pressure.

The results of our models are consistent with analogue experiments of the 'fault reactivation model', which show strong influence of rigid basement blocks (e.g., McClay and Buchanan 1992, Buchanan and McClay 1991). Our experimental set-up differs from that

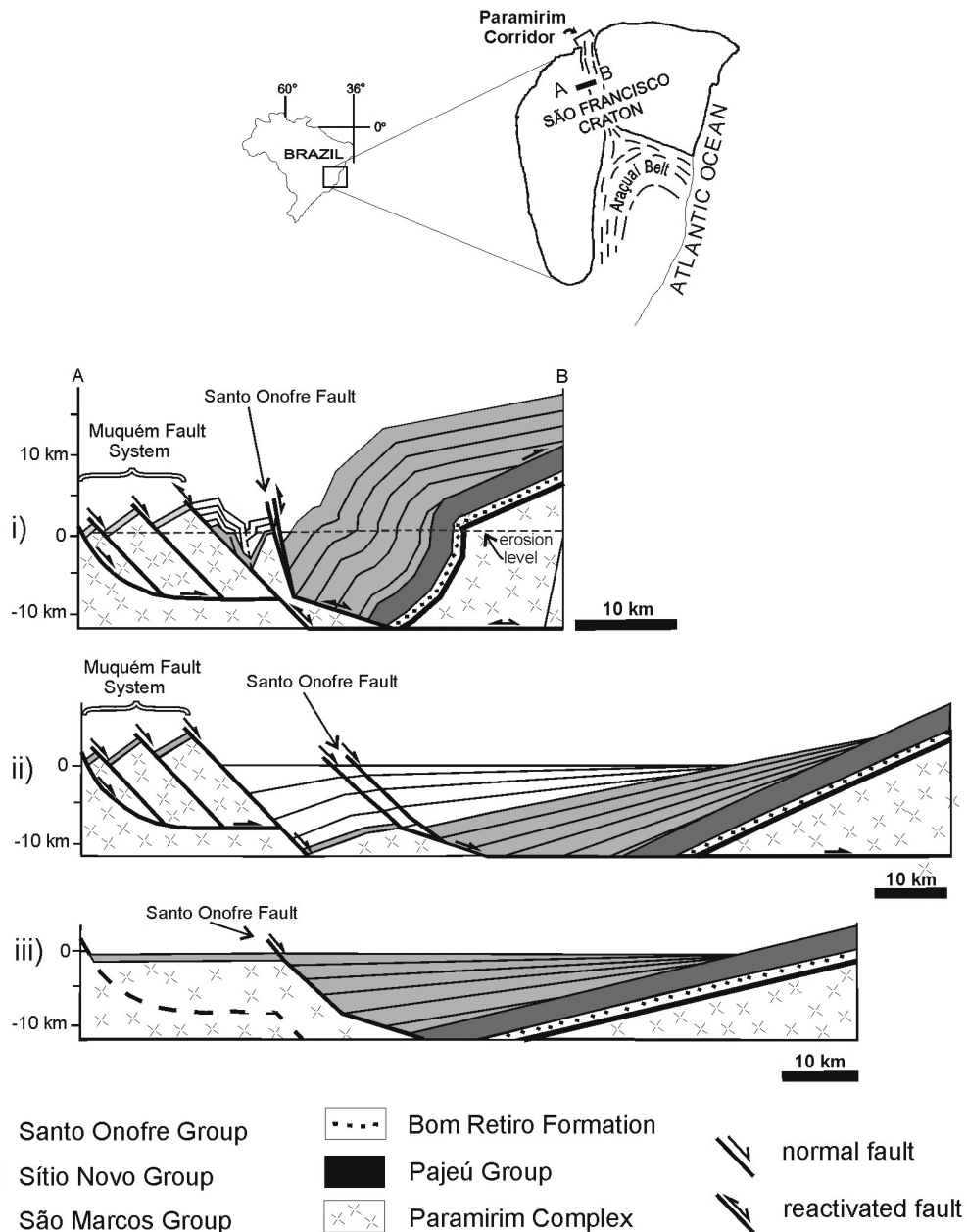


Fig. 14 – (i) Balanced cross-section of the northern Serra do Espinhaço Range, eastern margin of the São Francisco Craton, Brazil (see inset for localization), illustrating an inversion process with a concave-up backstop (modified from Abad Posada, unpublished data). Note reactivation of normal detachments, shearing backward and strong counterclockwise rotation of the Sítio Novo Group. (ii) Pre-inversion and (iii) pre-extension geometries are also shown. Balanced section calculation suggests a total contraction of 48%.

of Buchanan and McClay (1991) by the shape of the curved backstop geometry and by a smaller sand pack thickness. Under their conditions, analogue models always produced reactivation of the main listric extensional detachment and of the normal faults of the crestal

collapse graben. In addition, footwall shortcut thrusts may be produced as well as hanging wall backthrusts at the footwall toe. Our experiments demonstrated that the backstop geometry exerts a strong control on the normal detachment reactivation. We found that whilst

a concave-up backstop may generate reactivation from 40% of shortening on, a convex-up backstop does not produce any normal detachment reactivation until 60% of shortening.

#### *The buttress*

Our experimental models, performed with stiff normal footwalls, produced counterclockwise rotation of the syn-rift sequence in the contractional foreland due to the presence of a 70°-dip normal detachment cut-off angle. We presume that a 60°-dip normal footwall with a high frictional basal detachment may produce the same result.

As with the backward movement, the buttress-effect is rarely described in inversion tectonics. Rotation of the syn-rift pack was related to a buttress effect by de Graciansky et al. (1989) along the Gourdan-Vial reverse fault, in the Western Maritime Alps. Bailey et al. (2002) studied the Tye River fault zone in the Appalachian Blue Ridge Province and concluded that, during inversion, a basement-cored extensional footwall acted as a buttress and controlled folding in the cover sequence.

#### IMPLICATIONS

Backward movement in contractional environments is commonly described as a buttress effect (the thrust-sheet dislocation restrains due to a rigid mass in the foreland), but as demonstrated by Bonini et al. (1999), it may depend on the backstop geometry. Eisenstadt and Sims (2005) call attention to the fact that, in sand models, both in contraction and in inversion, regardless to the boundary conditions, the shortening is accommodated by sand pack rising bounded by a fore- and a backthrust. Thus, our experimental models demonstrated that the backstop geometry does not modify overall deformation structures, but controls the predominant extrusion sense and, as a consequence, the normal detachment reactivation.

The backstop height controls backward movement *versus* vertical strain, but does not interfere in the forward movement or reactivation of pre-existent normal detachment. Finally, the comparison with Buchanan and McClay's (1991) experiments suggests that the reactivation of pre-existent normal detachment is more dependent on sand pack height than on backstop height.

#### CONCLUSION

In our analogue sand models that simulated the inversion of a half-graben using stiff undeformable footwall blocks and stiff backstops of different geometry, the following features were detected:

- a) a convex-up backstop produces the ejection of the sedimentary sequence to the hinterland, and until 60% of shortening no reactivation of the extensional detachment takes place;
- b) a concave-up backstop also generates a strong ejection to the hinterland, but forward propagating movement leading to detachment reactivation may take place after 40% of shortening;
- c) a vertical backstop, regardless to its height, produces normal detachment reactivation after 20% of shortening;
- d) a high (70°) normal detachment cut-off angle causes pronounced rotation of the syn-rift sequence in the inversional foreland.

The results suggest that the reactivation of a normal detachment in inversion tectonics is strongly influenced by the backstop geometry. In the reactivation process, the backstop height is a negligible factor. We conclude that different backstop geometries may modify the common shortening process that is usually accommodated by a pop-up type structure with equal slip on fore- and backthrust. In addition, we conclude that a stiff high angle footwall leads to a buttress effect in the syn-rift sequence.

#### ACKNOWLEDGMENTS

We wish to thank the financial support from Conselho Nacional de Desenvolvimento Científico and Tecnológico (CNPq) (process no. 477157/2003-3) and from Fundação de Amparo à Pesquisa do Estado de Minas Gerais (FAPEMIG) (CRA 871/06). We are greatly indebted to the reviewers for their careful revision and constructive comments, which greatly improved our work.

#### RESUMO

O estilo da deformação de sequências sedimentares de bacias submetidas a uma inversão tectônica positiva foi discutido a partir da análise de modelos laboratoriais, desenvolvidos em

caixas de experimentos, com camadas de areia depositadas no espaço entre dois blocos de madeira. O espaço simulava estágios de extensão crustal que conduziram à formação de (1) um hemi-graben, gerado sobre um descolamento basal listrico, com os blocos simulando o teto e o muro; e (2) um graben, com os blocos representando as margens externas que se distanciaram ao longo de um descolamento horizontal. Combinações de dois ângulos diferentes foram usadas para simular o mergulho das falhas normais curvas ao longo da face interna dos blocos de madeira. Nos hemi-grabens, os anteparos possuíam geometria convexa, e, nos grabens, geometria côncava. No pacote de areia, o encurtamento foi particionado em movimentos dirigidos a pós e antepais, e a cinemática da contração foi fortemente influenciada pela geometria convexa ou côncava das faces internas dos anteparos. Um efeito obstáculo, caracterizado por rotação do pacote de areia, próximo ao bloco do muro, foi mais elevado junto às faces internas dos blocos de mais alto ângulo de mergulho. Os resultados foram comparados a outros experimentos físicos e aplicados a uma bacia invertida encontrada na natureza.

**Palavras-chave:** modelos analógicos, geometria do anteparo, efeito obstáculo, tectônica de inversão, reativação do descolamento basal.

#### REFERENCES

- BAILEY CM, GIORGIS S AND COINER L. 2002. Tectonic inversion and basement buttressing: an example from the Appalachian Blue Ridge province. *J Struct Geol* 24: 925–936.
- BEAUMONT C, FULLSACK P AND HAMILTON J. 1994. Styles of crustal deformation in compressional orogens caused by subduction of the underlying lithosphere. *Tectonophysics* 232: 119–132.
- BONINI M, SOKOUTIS D, TALBOT CJ AND BOCCALETTI M. 1999. Indenter growth in analogue models of Alpine-type deformation. *Tectonics* 18: 119–128.
- BRUN J-P AND NALPAS T. 1996. Graben inversion in nature and experiments. *Tectonics* 15: 677–687.
- BUCHANAN PG AND MCCLAY KR. 1991. Sandbox experiments of inverted listric and planar fault systems. *Tectonophysics* 188: 97–115.
- BUTLER RWH. 1989. The influence of pre-existing basin structure on thrust system evolution in the Western Alps. In: COOPER MA AND WILLIAMS GD (Eds), *Inversion Tectonics*. Geol Soc London Spec Pub 44: 105–122.
- BYRNE DE, WANG W AND DAVIS M. 1993. Mechanical role of backstops in the growth of forearcs. *Tectonics* 12: 123–144.
- COBBOLD PR, DURAND S AND MOURGUES R. 2001. Sandbox modelling of thrust wedges with fluid-assisted detachments. *Tectonophysics* 334: 245–258.
- COOPER MA, WILLIAMS GD, DE GRACIANSKY PC, MURPHY RW, NEEDHAM T, DE PAOR D, STONELEY R, TODD SP, TURNER JP AND ZIEGLER PA. 1989. *Inversion Tectonics – a discussion*. In: COOPER MA AND WILLIAMS GD (Eds), *Inversion Tectonics*. Geol Soc London Spec Pub 44: 335–347.
- DE GRACIANSKY P, DE DARDEAU G, LEMOINE M AND TRICART P. 1989. The inverted margin of the French Alps. In: COOPER MA AND WILLIAMS GD (Eds), *Inversion Tectonics*. Geol Soc London Spec Pub 44: 105–122.
- EISENSTADT G AND SIMS D. 2005. Evaluating sand and clay models: do rheological differences matter? *J Struct Geol* 27: 1399–1412.
- GLEN RH, HANCOCK PL AND WHITTAKER A. 2005. Basin inversion by distributed deformation: the southern margin of the Bristol Channel Basin, England. *J Struct Geol* 24: 2113–2134.
- GLENNIE KW AND BOEGNER PL. 1981. Sole Pit Inversion Tectonics. In: ILLING LV AND HOBSON GD (Eds), *Petrol Geol Cont Shelf Northwest Europe*, p. 110–120.
- GOMES CJS. 1996. O papel do anteparo na modelagem física de cinturões compressivos – um estudo aplicado a um duplex do tipo pilha antiformal. *Geonomos* 4: 51–60.
- HAYWARD AB AND GRAHAM RH. 1989. Some geometrical characteristics of inversion. In: COOPER MA AND WILLIAMS GD (Eds), *Inversion Tectonics*. Geol Soc London Spec Pub 44: 17–39.
- HUBBERT MK. 1937. Theory of scale models as applied to the study of geological structures. *Geol Soc Am Bul* 48: 1459–1520.
- JADOON IAK, LAWRENCE RD AND LILLIE RJ. 1994. Seismic data, geometry, evolution and shortening in the active Sulaiman Fold-and-Thrust Belt of Pakistan, southwest of the Himalayas. *Am Ass Petrol Geol Bull* 78: 758–774.
- MCCLAY KR. 1989. Analogue models of inversion tectonics. In: COOPER MA AND WILLIAMS GD (Eds), *Inversion Tectonics*. Geol Soc London Spec Pub 44: 41–59.
- MCCLAY KR. 1990. Extensional fault systems in sedimentary basins: a review of analogue model studies. *Marine Petrol Geol* 7: 206–233.
- MCCLAY KR. 1995. The geometries and kinematics of inverted fault systems: a review of analogue model studies. In: BUCHANAM JG AND BUCHANAM PG (Eds), *Basin Inversion*. Geol Soc London Spec Publ 88: 97–118.

- MCCLAY KR AND BUCHANAN PG. 1992. Thrust faults in inverted extensional basins. In: MCCLAY KR (Ed), Thrust Tectonics, London: Chapman and Hall, p. 93–104.
- MITRA S. 1988. Three dimensional geometry and kinematic evolution of the Pine Mountain thrust system, southern Appalachians. Bull Geol Soc Am 100: 72–95.
- MULUGETA G. 1988. Modelling the geometry of Coulomb thrust wedges. J Struct Geol 10: 847–859.
- MULUGETA G AND KOYI H. 1987. Three-dimensional geometry and kinematics of experimental piggyback thrusting. Geology 15: 1052–1056.
- PANIEN M, SCHREURS G AND PFIFFNER A. 2005. Sandbox experiments on basin inversion: testing the influence of basin orientation and basin fill. J Struct Geol 27: 433–445.
- ROSSETTI F, FACCENNA C AND RANALLI G. 2002. The influence of backstop dip and convergence velocity in the growth of viscous doubly-vergent orogenic wedges: insights from thermomechanical laboratory experiments. J Struct Geol 24: 953–962.